

# Remaining Useful Life Prediction with Uncertainty Quantification of Liquid Propulsion Rocket Engine Combustion Chamber<sup>\*</sup>

Soha Kanso<sup>\*</sup> Mayank S. Jha<sup>\*</sup> Marco Galeotta<sup>\*\*</sup>  
Didier Theilliol<sup>\*</sup>

<sup>\*</sup> *Centre de Recherche en Automatique de Nancy (CRAN), UMR 7039, CNRS*

*University of Lorraine, 54506 Vandoeuvre-lès-Nancy Cedex, France*

<sup>\*\*</sup> *Centre national d'études spatiales (CNES), Launchers' Directorate, 52 rue Jacques Hillairet, 75612 Paris Cedex, France*

soha.kanso@univ-lorraine.fr, mayank-shekhar.jha@univ-lorraine.fr,  
marco.galeotta@cnes.fr, didier.theilliol@univ-lorraine.fr

---

**Abstract:** Reduction of spaceflight costs calls for development of new technologies that render rockets reusable. This new requirement and the continuous improvement of rocket engines require pro-active approach towards the possibility of integrating health monitoring systems on-board. These health monitoring strategies should also take into consideration the state of degradation and the remaining useful life prediction. In this paper, an Extended Kalman Filter is used to estimate the state of health and the dynamics of the degradation, and the remaining useful life is predicted with respect to failure thresholds pre-set by the user. The first-order inverse reliability method is employed to assess the quality of the remaining useful life prediction by quantifying the associated uncertainty. The overall method is validated using simulation study involving degradation data provided by Centre National d'Etudes Spatiales (CNES) applied to liquid propulsion rocket engine (LPRE) combustion chamber.

*Keywords:* Remaining Useful Life – Prognostic – Liquid Propulsion Rocket – Extended Kalman Filter – Inverse First Order Reliability Method.

---

## 1. INTRODUCTION

The reuse of liquid propulsion rocket engine (LPRE) has become increasingly important in order to reduce the cost as well as wastage of materials (Kawatsu (2019)). This new requirement and the recent interest to improve the performance and reduce load, has led to reflections on the possibilities of considering on-board engine health monitoring systems. Such monitoring systems should take into account estimation of health of the motor as well as prediction of remaining useful life (RUL) (Dai et al. (2013)).

Therefore, the necessity of an accurate and efficient health management system has become extremely important in the context of safety and mission-critical engineering systems. The objective of health monitoring is to survey the performance of these systems continuously, perform diagnostics at the system or subsystem level, perform prognostics at the component / system level, and support online decision (Sikorska et al. (2011)). Approaches based on measurement information of health state are divided into the following categories :

- **Model-based:** An empirical or physical model of the degradation is used to assess health state. However, building models is not a simple task as the degradation processes are not generally understood well (Sikorska et al. (2011));
- **Data-driven:** These approaches are primarily based on data and do not require accurate model of system or degradation process (Tsui et al. (2015));
- **Hybrid:** These approaches combine the advantages of the two methods above. The information provided by the real sensor measurements are merged with an approximately correct degradation model in an appropriate manner (Jha et al. (2016a))(Simon et al. (2014)). This approach has been applied later in this paper.

Prognostics allows for predicting of future failures and RUL. Uncertainty evaluation and management are important aspects of health monitoring due to the presence of several unknown factors that affect the functioning of the concerned system. There are two main categories of methods for uncertainty quantification (Sankararaman and Goebel (2013)): sampling-based methods and analytical methods.

In sampling-based methods such as Monte Carlo simulations, a large number of random realizations of *RUL*

---

<sup>\*</sup> This work was supported by Centre National d'Etudes Spatiales (CNES).

are generated. Monte Carlo sampling (MCS) approximate the entire probability distribution. These methods require considerable time for online implementation. Furthermore, MCS based methods use random samples for uncertainty quantification, and therefore do not guarantee generation of exactly same result while using the same algorithm. This work considers application of the analytical method Inverse First Order Reliability Method (IFORM) that allows for quantification the RUL uncertainty through generation of a confidence interval. IFORM enables calculation of RUL value for a given probability and remains well suitable for linear or linearized systems under the setting of linear stochastic Gaussian filter such as Kalman filter and Extended Kalman filter (EKF). Moreover, IFORM is computation efficient and remains feasible for implementation in real time. Another advantage of this approach is that it can produce deterministic results i.e. the same PDF (Probability Distribution Function) can be produced every time the algorithm is executed leading to repeatable results and thus facilitating verification and validation protocols in the aerospace domain (Sankararaman et al. (2014)).

This paper extends the previous work (Chelouati et al. (2021)) with formulation of RUL prediction problem as a hybrid prognostics procedure and presents IFORM as a suitable method for quantification of uncertainty on RUL predictions. The novelty lies in quantification of uncertainty and application of IFORM in the context of LRPE. To that end, Section 2 presents a brief description of the liquid propellant engine adopted in a previous study (Chelouati et al. (2021)). Section 3 presents the estimation of the State Of Health (SoH) and its evolution in the future by using an appropriate degradation model and a linear stochastic filter (Bressel et al. (2016a)). Section 4 presents the RUL prediction algorithm wherein predictions generated at each instant of time using futuristic projections as well as an appropriate analytical expression. Section 5 describes the IFORM algorithm, which is used for uncertainty quantification. In section 6, methods are applied on dataset generated by the dynamic simulator (CARINS) developed by the CNES, and finally, section 7 presents the conclusions.

## 2. LIQUID PROPULSION ROCKET ENGINE

### 2.1 System description

A fictive Liquid oxygen oxidizer - Liquid hydrogen fuel (LOX-LH2) engine of 10 kN thrust with a chamber propellant supply via two electro-pumps is chosen as a practical application case for RUL estimation methods. The chamber is equipped with a hydrogen regenerative circuit (RC) and a nozzle allowing to deliver the required thrust of 10 kN. Two isolation valves VCO and VCH are located on the propellants feed lines. They enable to admit the propellants into the chamber. The operating range of thrust is between 50 and 110 % of the nominal thrust. To provide data that can be used in the RUL prediction algorithms, typical engine life profiles have been simulated corresponding to two types of engines in open loop:

- Qualification (or production support) engines

- Flight engines

Qualification engines have more diverse usage profiles that cover multiple operating points, while flight engines have only two operating points. The RUL of the latter will be studied in this work. All the data were generated from the dynamic simulator system realized with the tool CARINS by the CNES (Chelouati et al. (2021)).

### 2.2 Degradation description and modeling

Strong thermomechanical solicitation on the internal wall of the chamber causes several cracks responsible for a direct leakage of cold hydrogen into the chamber by creating a cooling film on the internal wall (Hötte et al. (2020)). This presence of film cooling leads to a low heat flux extracted by the CR and an inhomogeneity of mixture ratio (MR) in the chamber, which can be observed macroscopically with a loss of combustion efficiency, leading to an overall degradation of the engine performance. In a previous study, it was identified that among the measured process data, the characteristic velocity efficiency  $\eta C^*$  would be the most appropriate candidate to be the state of health indicator (SoH). Once cracking appears,  $\eta C^*$  starts to decrease.

This work mainly focuses on the degradation dynamics as the global system model is not available. The measurement data under degradation is considered to analyse the degradation dynamics. Degradation processes exhibit certain prominent characteristics such as monotonicity with time and stochasticity. As such, various mathematical functions can be considered as viable candidate for modelling of degradation dynamics (Jha et al. (2016b)). In this paper, the evolution of health indicator is assumed to be modeled according to the following exponential mathematical formulation:

$$f(t) = e^{\alpha t} + f_0 \quad (1)$$

where  $f_0$  is the degradation value at time  $t = 0$  and  $\alpha$  is the degradation progression parameter (unknown parameter). In order to estimate the state of health  $f(t)$  and the degradation evolution  $\alpha$ , a hybrid approach which is the EKF is applied in the following section.

## 3. SOH ESTIMATION

### 3.1 Problem formulation

Under linear and additive Gaussian conditions, the EKF can be used to evaluate the state estimation that minimizes the mean square error. The dynamics of the EKF are generated by consecutive cycles of prediction and filtering (Chelouati et al. (2021)).

In this context of state and parameter estimation, the system is described in discrete time using Euler order 1:

$$f(k) = g(f(k-1), \alpha(k-1), k) + w_f(k) \quad (2)$$

where  $f(\cdot)$  is the unknown SoH,  $g(\cdot, \cdot, k)$  is the non-linear transition function allowing to obtain the current state through the previous states and  $w_f$  is the additive Gaussian process noise associated to  $f(\cdot)$  with variance  $\sigma_f$ . In comparison to the global system dynamics, the degradation progression rate is considered slow and modelled as a random walk process:

$$\alpha(k) = \alpha(k-1) + w_\alpha(k) \quad (3)$$

where  $w_\alpha$  is an additive noise associated to  $\alpha$  with variance  $\sigma_\alpha$ . Then, the discrete equations (2) and (3) can be written in the linearized state form as:

$$x(k+1) = A(k)x(k) + w(k) \quad (4)$$

where  $x(k) = \begin{bmatrix} f(k) \\ \alpha(k) \end{bmatrix}$ ,  $A(k) = \begin{bmatrix} 1 + \alpha(k).T_s & -f_0.T_s \\ 0 & 1 \end{bmatrix}$  is the Jacobian matrix with  $T_s$  as the sampling time and  $w(k) = \begin{bmatrix} w_f(k) \\ w_\alpha(k) \end{bmatrix}$ .

The observations of the state of this system are done according to the following observation equation:

$$z(k) = h(x(k), k) + v(k) \quad (5)$$

where  $z(k)$  is the measurement at instant  $k$ ,  $v(k)$  is the additive observation noise with variance  $\sigma_v$ , and  $h(\cdot)$  is the observation function. The noises  $w(k)$  and  $v(k)$  are assumed to be Gaussian with zero mean and variances  $Q$  and  $R$  respectively with  $Q = \begin{bmatrix} \sigma_f^2 & 0 \\ 0 & \sigma_\alpha^2 \end{bmatrix}$  and  $R = \sigma_v^2$ .

### 3.2 SoH estimation based on EKF

The EKF (Durrant-Whyte (2006)) handles the nonlinearity of system and measurements and allow to estimate the unknown parameters. The discrete EKF algorithm (Algorithm 1) comprises three steps which are presented as a pseudo-algorithm with  $E(\cdot)$  as the mean operator and  $Var(\cdot)$  as the variance operator.

---

#### Algorithm 1 SoH Estimation using EKF

---

**Input :**  $\hat{x}(0|0)$ ,  $P(0|0)$ ,  $z(0)$ ,  $Q$ ,  $R$   
**Output :**  $\hat{x}(k)$ ,  $P(k|k)$

##### Initialization

$\hat{x}(0|0) = E(x_{t_0})$ ,  $P(0|0) = Var(x_{t_0})$

##### Prediction

$\hat{x}(k|k-1) = A(k)\hat{x}(k-1|k-1)$   
 $P(k|k-1) = A(k)P(k-1|k-1)A^T(k) + Q$

##### Correction

$\hat{x}(k|k) = \hat{x}(k|k-1) + W(k)[z(k) - h(\hat{x}(k|k-1))]$   
 $P(k|k) = P(k|k-1) - W(k)S(k)W^T(k)$   
 with  $W(k) = P(k|k-1)\nabla h_x^T(k)S^{-1}(k)$ ,  $\nabla h_x(k) = \frac{\partial h(k)}{\partial x(k)}$   
 and  $S(k) = \nabla h_x(k)P(k|k-1)\nabla h_x^T(k) + R$   
 $\hat{x}(k) \leftarrow \hat{x}(k|k)$

---

## 4. RUL ESTIMATION

Algorithm 1 computes at each discrete time the SoH and the degradation evolution which are used for RUL prediction. As shown in Fig. 1, the difference between the time of prediction  $t_{pred}$  and the predicted end of life  $t_{failure}$  is defined by the remaining useful life (Saxena et al. (2008)):

$$RUL(k) = t_{failure} - t_{pred} \quad (6)$$

RUL prediction can be done by two methods presented in the following sections.

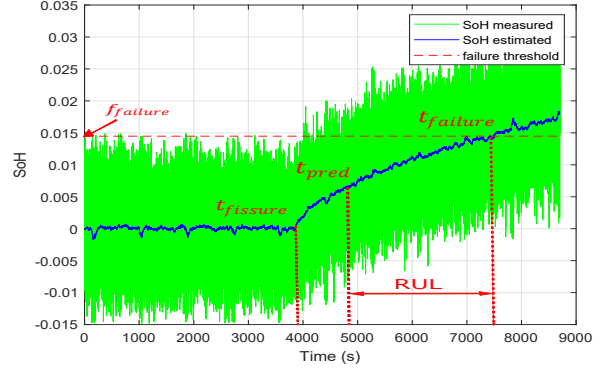


Fig. 1. RUL illustration

### 4.1 Using $p$ -step ahead prediction of RUL

The previous algorithm provides the estimated state of health  $\hat{f}(k)$  and its evolution  $\hat{\alpha}(k)$  at every discrete time  $k$ . This information serves as an input of the prediction algorithm detailed below (Algorithm 2). At each time  $k$ , the future SoH is predicted until it passes a threshold  $f_{failure}$  predefined by the user. The projection in the future is done using the estimated degradation model according to the following recurrence :

$$\hat{f}(k+p) \leftarrow [1 + \hat{\alpha}(k).T_s]\hat{f}(k+p-1) - f_0.T_s \quad (7)$$

This operation is repeated each time a new estimate of SoH is generated by Algorithm 1. The RUL obtained by Algorithm 2 is noted by  $RUL_{proj}$ .

---

#### Algorithm 2 $p$ -step ahead prediction of RUL

---

**Input :**  $\hat{f}(k)$ ,  $\hat{\alpha}(k)$ ,  $f_{failure}$   
**Output :**  $RUL_{proj}(k)$

**Initialization :**  $p \leftarrow 0$

**while**  $\hat{f}(k+p) < f_{failure}$  **do**

$\hat{f}(k+p) \leftarrow [1 + \hat{\alpha}(k).T_s]\hat{f}(k+p-1) - f_0.T_s$   
 $p \leftarrow p + T_s$

**end while**

$RUL_{proj}(k) \leftarrow p$

---

### 4.2 Using analytic expression

Under the assumptions of linearity, the prediction of RUL can be done analytically by expliciting the expression of RUL.

$$\hat{f}(k+1) = (1 + \hat{\alpha}(k).T_s)\hat{f}(k) - f_0.T_s.\hat{\alpha}(k)$$

By successive recurrence until time  $k+p$  with  $f_0 = 0$  :

$$\hat{f}(k+p) = (1 + \hat{\alpha}(k).T_s)^p \hat{f}(k)$$

where  $p$  is the number of time steps until threshold is reached.

For  $\hat{f}(k+p) = f_{failure}$ ,  $RUL_{cal}(k)$  is given by :

$$RUL_{cal}(k) = p.T_s = \frac{\ln(f_{failure}) - \ln(\hat{f}(k))}{\ln(1 + \hat{\alpha}(k).T_s)}.T_s \quad (8)$$

The function  $RUL_{cal}$  takes as input the estimated values of  $\hat{f}$  and  $\hat{\alpha}$  at time  $k$ . This expression will be used in the section below for uncertainty quantification.

## 5. RUL UNCERTAINTY QUANTIFICATION BASED ON IFORM

### 5.1 RUL uncertainty

It is not only necessary to build a robust algorithm for diagnosis and prognosis but it is also important to quantify the degree of confidence in the prognostic results. Performing such uncertainty quantification online is necessary to aid decision-making process.

The predicted RUL at time  $k$  depends of several factors (Sankararaman et al. (2014)). Let  $X = [X_1, X_2, \dots, X_i, \dots, X_n]$  be the vector of all such factors, where  $n$  is the number of uncertain quantities influencing the prediction of RUL. Then,  $RUL$  can be expressed in terms of any non-linear function  $R$  as:

$$RUL = R(X) \quad (9)$$

The quantities in  $X$  are considered uncertain, and the objective is to calculate their combined effect on the prediction of RUL. This task can be achieved by computing the probability density function or the cumulative distribution function of RUL.

### 5.2 Inverse First-Order Reliability Method (IFORM)

The IFORM algorithm necessitates a limit state function  $R(X)$  that represents the boundary between the safe and the failure zone in the random variable Standard Normal Space as shown in Fig. 2 where  $U_1$  and  $U_2$  correspond to the random state variables  $X_1$  and  $X_2$  in the standard normal space, and  $u_1$  and  $u_2$  are the realizations of  $U_1$  and  $U_2$  (Bressel et al. (2016b)), (Sankararaman et al. (2014)).

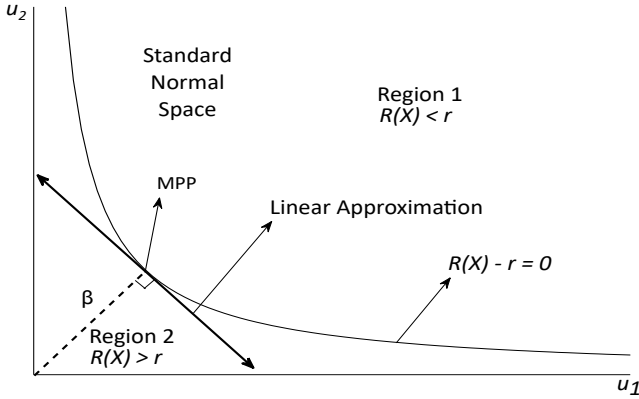


Fig. 2. Limit state function and MPP (Sankararaman et al. (2014))

Therefore, it is important to find a linear function that resembles the contour  $R(x) - r = 0$ . The linearization point must be on this demarcation curve; in other words, it must satisfy  $R(x) - r = 0$ . However, there exist infinite points that satisfy this condition. Each of these infinite points has a likelihood of occurrence, and the one with the maximum likelihood of occurrence is adopted as a linearization point and it's called MPP (Most Probable Point). The distance between MPP and the origin is exactly equal to  $\beta$  (reliability index) and since :

$$P(R \leq r) \approx \Phi(-\beta) \quad (10)$$

where  $\Phi(\cdot)$  represents the standard normal cumulative distribution function, the problem of computing CDF is reduced to identify the MPP on the limit state curve using the iterative procedure Algorithm 3 where  $\mu_i = [\hat{f}(k), \hat{\alpha}(k)]$  and  $\sigma_i = [P(k|k, 1), P(k|k, 2)]$ .

---

#### Algorithm 3 IFORM for RUL estimation

---

**Input :**  $\mu_i, \sigma_i, f_{failure}, \beta$

**Output :**  $RUL_{IFORM}$

---

**Initialization :**

$j \leftarrow 0$

$x_i^j \leftarrow [x_1^j, x_2^j]$

▷ Initial guess of MPP

**while**  $|R(x_i^j) - r| \leq \delta_1$  **and**  $|x_i^{j+1} - x_i^j| \leq \delta_2$  **do**

▷ Tolerance limits  $\delta_1$  and  $\delta_2$

$u_i \leftarrow (x_i - \mu_i) / \sigma_i$

$a_i \leftarrow \frac{\partial R}{\partial u_i} = \frac{\partial R}{\partial x_i} \frac{\partial x_i}{\partial u_i}$

$w^{j+1} \leftarrow \frac{a}{|a|} \beta$

$x_i^{j+1} \leftarrow u_i \cdot \sigma_i + \mu_i$

**end while**

$RUL_{IFORM} \leftarrow R(x_i^{j+1})$

---

This iterative procedure described usually converges within 4 or 5 iterations. One of the practical challenges of IFORM method is that it requires an explicit expression of RUL i.e. an explicit function  $RUL = R(X)$  which could be difficult in the case of complex systems.

## 6. SIMULATION RESULTS AND DISCUSSION

As noted in section 2.2,  $\eta C^*$  provided by the LPRE simulator is considered the indicator of state of health SoH. In the following, a change of scale was done to have a degradation evolution consistent with the expectations of used methods :

$$f_{mes}(k) = \frac{\eta C_{max}^* - \eta C^*(k)}{\eta C_{max}^* - \eta C_{min}^*} \quad (11)$$

with  $\eta C_{max}^*$  and  $\eta C_{min}^*$  are respectively the maximum and the minimum value of  $\eta C^*$ .  $f(\cdot)$  represents the state of health indicator and therefore it is denoted as SoH.

The first step in the EKF algorithm is the initialization of the states and the adjustment of the covariance matrices to make the filter work properly. Since  $z(\cdot)$  represents the measured value of SoH ( $z(k) = f_{mes}(k)$ ), the average of the first measurements can be taken as the initial value of state :

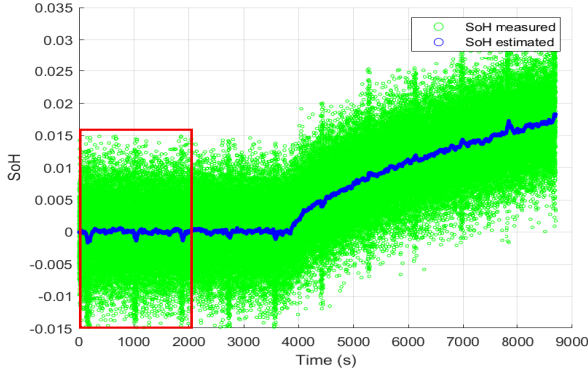
$$\hat{f}(0|0) = \frac{1}{500} \sum_{i=1}^{500} z(i) \approx 0 \text{ and } \hat{\alpha}(0|0) = 0$$

In practice, process and measurement noise  $Q$  and  $R$  are difficult to obtain. The steady-state performance of the filter is determined by the values of the state and observation noise covariances which are chosen as the filter inputs. There are some general principles to be considered when tuning as referred in Durrant-Whyte (2006). In this study,  $Q$  and  $R$  are set as :

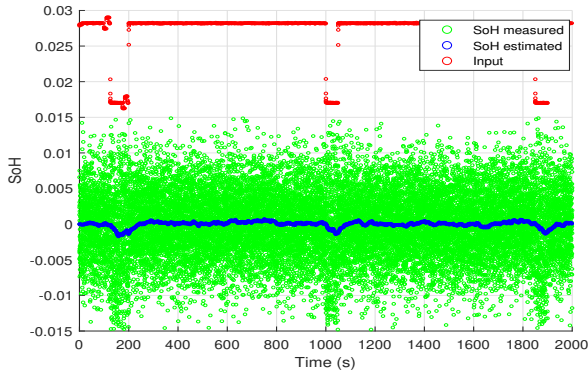
$$Q = \begin{bmatrix} \sigma_f^2 & 0 \\ 0 & \sigma_\alpha^2 \end{bmatrix}, R = \sigma_v^2$$

with  $\sigma_f = 3.10^{-5}$ ,  $\sigma_\alpha = 10^{-6}$ ,  $\sigma_v = 8.10^{-3}$

The measured and estimated SoH for about 10 launches and landing are presented in Fig. 3a. A strong correlation



(a) SoH estimation based on EKF



(b) Variation of the operating points

Fig. 3. Estimation of SoH

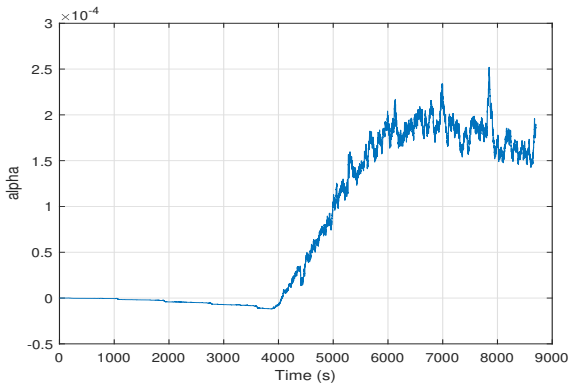


Fig. 4. Estimation of parameter  $\alpha$

is observed between the two curves, which implies that the EKF is able to estimate the degradation of the indicator of SoH since the estimated values converge to the measured values. Fig. 3b illustrates the variation of the operating points of flight engine. At  $t \approx \{125s, 1000s, 1850s\}$ , the system functions with 60% of the nominal thrust for about 80s and this appears via the peaks in the measured and the estimated curves of SoH. Fig. 4 shows the estimated  $\hat{\alpha}$ , a fast evolution of the slope occurs after the appearance of cracking and tends toward a maximum. The importance of  $\hat{\alpha}$  is to provide information on the speed of degradation. A tendency analysis applied on  $\hat{\alpha}$  can be developed to detect the occurrence of faults and to activate the RUL prediction process.

Assuming that the degradation is only influenced by one degradation mode (operating condition), the  $RUL_{real}$  allows to validate the RUL predictions and is calculated by subtracting the prediction time from the failure time. The RULs generated by projection ( $RUL_{proj}$  of Algorithm 2) and by explicit expression ( $RUL_{cal}$  of Eq.(8)) are plotted and compared with theoretical RULs ( $RUL_{real}$ ) and its  $\pm 10\%$  bounds in order to check the robustness of the predictions. Note that the RUL prediction procedure is launched at the time of appearance of cracking to avoid computational complexities at the beginning of the degradation. Fig. 5 shows that the  $RUL_{proj}$  is merged with the  $RUL_{cal}$ . In fact,  $RUL_{cal}$  is computed to apply IFORM method for uncertainty quantification. Furthermore, the RULs are overestimated for the first 1000 s, this is explained by the time the algorithm takes to converge to the  $RUL_{real}$  curve. Once the estimated RUL converges to the  $RUL_{real}$ , it remains in the  $\pm 10\%$  range. For  $t \approx 7500s$ , the SoH exceeds the predetermined threshold and the RUL becomes zero.

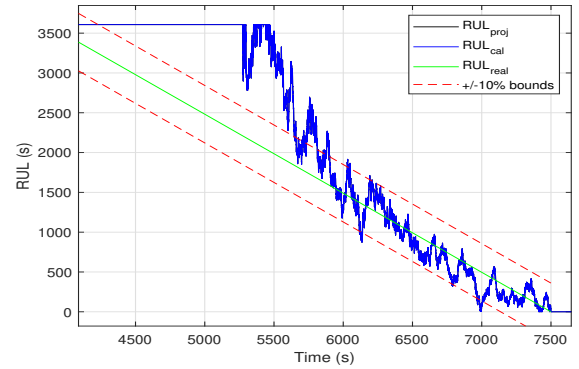


Fig. 5. RUL estimation

The IFORM method is directly applied to calculate the value of RUL corresponding to  $P(R \leq r) = [0.3, 0.5, 0.95]$  as presented in Fig. 6. Here,  $RUL_{IFORMP=0.3}$ ,  $RUL_{IFORMP=0.95}$  and  $RUL_{IFORMP=0.5}$  correspond respectively to 30%, 95% and 50% of the RUL probability distribution. At any time  $t$ , the two curves  $RUL_{IFORMP=0.3}$  and  $RUL_{IFORMP=0.95}$  constitute 65% of the RUL distribution by generating the 30% and 95% bounds over the distribution. Moreover,  $RUL_{IFORMP=0.5}$  is plotted to indicate the median of the RUL. The bounds and the median are calculated until  $t_{failure} = 7500s$ , when the failure looks imminent. According to Fig. 6, it is seen that the uncertainty of RUL distribution is initially large (high variance of RUL PDF) which progressively decreases until the failure is reached. The latter indicates decrease in the inherent uncertainty of RUL PDF which is desirable for accurate predictions.

The RUL uncertainty at initial stages is large owing to large prediction time horizon calling for incorporation of uncertainty associated with future states over longer periods of time, and initial estimation of inaccurate  $\alpha$  with large variance. However, at a later time stages, as the estimation quality improves with in-coming measurements (sensor information) the inherent uncertainty of the RUL decreases.

Fig. 7 shows the computation time of IFORM algorithm

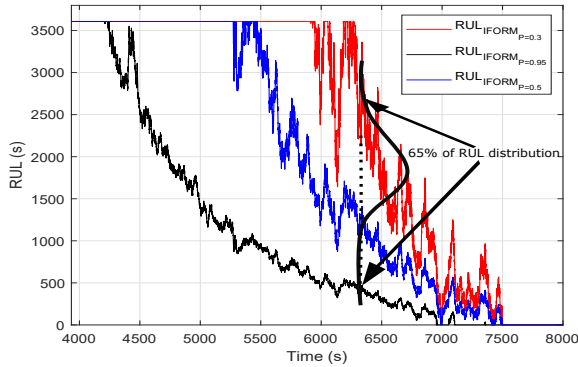


Fig. 6. Uncertainty quantification of RUL by IFORM

that converges approximately after a time of order  $10^{-5}$ s throughout the degradation process indicating a good possibility of online implementation of this approach online as well as within a closed loop.

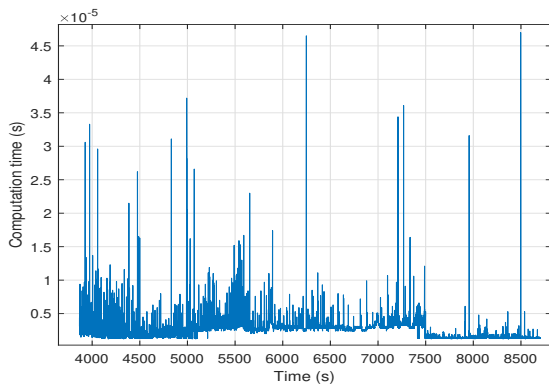


Fig. 7. Computation time of IFORM

## 7. CONCLUSION

This paper employs a hybrid approach for RUL predictions wherein knowledge brought in by an approximately correct degradation model is combined with sensor information to estimate the state of health of the LRPE as well as prediction of RUL. The methodology used is based on the Extended Kalman Filter (EKF) that leads to estimation the current health state and its evolution rate and consequently, allows for fast and accurate estimation of the RUL. The inherent uncertainty associated with RUL predictions of LRPE is quantified by generation of confidence bounds using IFORM approach that allows for calculation of RUL values corresponding to the specified user based probability levels. The procedure can be useful for online decision making. The obtained results demonstrate the efficacy of the presented approach for prediction of RUL of combustion chamber of LRPE for engines operating under nominal conditions. Future works will consider synthesizing a control law that adjust the performance of the system in order to minimize the risk of failure and to extend RUL.

## ACKNOWLEDGEMENTS

This work was supported by Centre National d'Etudes Spatiales (CNES).

## REFERENCES

- Bressel, M., Hilaret, M., Hissel, D., and Bouamama, B.O. (2016a). Extended kalman filter for prognostic of proton exchange membrane fuel cell. *Applied Energy*, 164, 220–227.
- Bressel, M., Hilaret, M., Hissel, D., and Bouamama, B.O. (2016b). Remaining useful life prediction and uncertainty quantification of proton exchange membrane fuel cell under variable load. *IEEE Transactions on Industrial Electronics*, 63, 2569–2577.
- Chelouati, M., Jha, M.S., Galeotta, M., and Theilliol, D. (2021). Remaining useful life prediction for liquid propulsion rocket engine combustion chamber. In *2021 5th International Conference on Control and Fault-Tolerant Systems (SysTol)*, 225–230.
- Dai, J., Das, D., Ohadi, M., and Pecht, M. (2013). Reliability risk mitigation of free air cooling through prognostics and health management. *Applied Energy*, 111, 104–112.
- Durrant-Whyte, H.F. (2006). Introduction to estimation and the kalman filter. *Semantic Scholar*.
- Hötte, F., Sethe, C.V., Fiedler, T., Haupt, M.C., Haidn, O.J., and Rohdenburg, M. (2020). Experimental lifetime study of regeneratively cooled rocket chamber walls. *International Journal of Fatigue*, 138, 105649.
- Jha, M.S., Bressel, M., Ould-Bouamama, B., and Dauphin-Tanguy, G. (2016a). Particle filter based hybrid prognostics of proton exchange membrane fuel cell in bond graph framework. *Computers Chemical Engineering*, 95, 216–230.
- Jha, M.S., Dauphin-Tanguy, G., and Ould-Bouamama, B. (2016b). Particle filter based hybrid prognostics for health monitoring of uncertain systems in bond graph framework. *Mechanical Systems and Signal Processing*, 75, 301–329.
- Kawatsu, K. (2019). Phm by using multi-physics system level modeling and simulation for emas of liquid rocket engine. *IEEE Aerospace Conference*, 1–10.
- Sankararaman, S., Daigle, M.J., and Goebel, K. (2014). Uncertainty quantification in remaining useful life prediction using first-order reliability methods. *IEEE Transactions on Reliability*, 63, 603–619.
- Sankararaman, S. and Goebel, K. (2013). Remaining useful life estimation in prognosis: An uncertainty propagation problem. *AIAA Infotech at Aerospace (I at A) Conference*, 1–8.
- Saxena, A., Goebel, K., Simon, D., and Eklund, N. (2008). Damage propagation modeling for aircraft engine run to-failure simulation. *International Conference on Prognostics and Health Management*.
- Sikorska, J., Hodkiewicz, M., and Ma, L. (2011). Prognostic modelling options for remaining useful life estimation by industry. *Mechanical Systems and Signal Processing*, 25, 1803–1836.
- Simon, C., Theilliol, D., Sauter, D., and Orkisz, M. (2014). Remaining useful life assessment via residual generator approach - a soh virtual sensor concept. *2014 IEEE Conference on Control Applications (CCA)*.
- Tsui, K.L., Chen, N., Zhou, Q., Hai, Y., and Wang, W. (2015). Prognostics and health management: A review on data driven approaches. *Mathematical Problems in Engineering*, 2015, 1–17.